Study of the characteristics of concentration sensing based on FBG Fabry-Perot cavity*

WU Fei(吴飞), ZHU Guo-fang(朱国芳), and CHEN Xi(陈曦)**

College of Electrical Engineering, Yanshan University, Qinhuangdao 066004, China

(Received 6 November 2008)

Fiber Bragg grating Fabry-Perot (FBG F-P) cavity is used as the sensing model to measure the refractive index of the liquid solution. The cladding of the fiber, which is used as the F-P cavity, is etched by HF solution to enhance the sensitivity to the external refractive index. The experimental results show that with the concentration change of the external solution, the effective refractive index of etched fiber will change, thus the spectra of FBG F-P cavity will appear a spilt point. The relationship between the wavelength at spilt point and the effective refractive index of etched fiber is approximately linear, and also periodical. The sensing model is theoretically analyzed based on transfer matrix method, and the corresponding mathematic model is established.

Document code: A **Article ID:** 1673-1905(2009)02-0138-5

DOI 10.1007/s11801-009-8156-1

Solution concentration is one of main parameters to denote the solution characteristics. In recent years, fiber grating sensors have been gradually applied to the measurement of solution concentration and refractive index[1-3]. However, the transmission spectrum of long period fiber grating (LPG) is unstable and sensitive to temperature and strain highly, which leads to the serious cross sensitivity[4,5]. There are relative reports of refractive index sensing based on FBG[6-8], but the exhaustive theoretical analysis is lack.

In this paper, we investigate the reflective spectrum characteristics of FBG F-P cavity which is etched on fiber cladding. The results show that when the solution concentration varies, the effective refractive index of the etched fiber will also change, which leads to the split point shift in reflection spectra. Furthermore, the linearity and periodicity of split point shift are deduced. Accordingly, the solution refractive index can be measured by detecting the wavelength of split point.

There is a corresponding relationship between the concentration and the refractive index of solution at constant temperature, which can be obtained from the table[9].

Assume that the refractive indexes of core, cladding and solution are n_1, n_2 and n_3 respectively, the radius of core and cladding are a and b separately. The refractive index profile is illustrated in Fig.1.

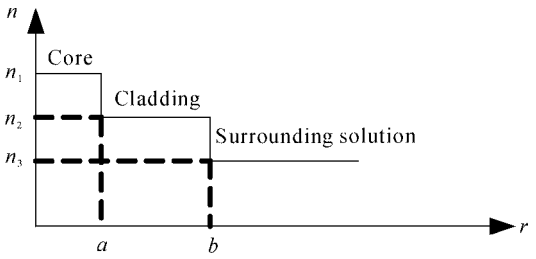

Fig.1 Refractive index profile of the fiber

For the single mode aixsymmetric fibers, only the model of LP_{01} and LP_{01} need to be considered. The characteristic equation is given by[10]

$$\frac{\left[\frac{J_0(u)}{uJ_1(u)}-\frac{K_0(\omega s)}{\omega s K_1(\omega s)}\right]\times\left[\frac{K_0(v)}{vK_1(v)}+\frac{I_0(\omega)}{\omega I_1(\omega)}\right]}{\left[\frac{J_0(u)}{uJ_1(u)}+\frac{I_0(\omega s)}{\omega s I_1(\omega s)}\right]\times\left[\frac{K_0(v)}{vK_1(v)}-\frac{K_0(\omega)}{\omega K_1(\omega)}\right]}=\frac{K_1(\omega)I_1(\omega s)}{K_1(\omega s)I_1(\omega)}, \tag{1}$$

where $u=a\sqrt{n_1^2k_0^2-\beta^2}$, $\omega=b\sqrt{\beta^2-n_2^2k_0^2}$, $v=b\sqrt{\beta^2-n_3^2k_0^2}$, $s=a/b$, $k_0=2\pi/\lambda$, J, I and K are the Bessel function of the first kind, the modified Bessel functions of the first and second kinds, respectively, and subscripts represent the order of the Bessel function.

For a given parameter fiber, the value of transmission coefficient β can be obtained by solving Eq.(1) at a specific

* This work has been supported by the National Nature Science Foundation of China (Grant No.60672015).

** E-mail:ysu-fbg@163.com

wavelength. Thus the effective refractive index n satisfies

$$n=\beta/k_0 . \tag{2}$$

The parameters of the fiber we used are shown as follows: λ_B=1549.945 nm, a =3.04 μm , n_1=1.451, n_2=1.444, hence, the effective refractive index of fundamental mode varies with both n_3 and b, namely, $n=f(n_3,b)$.

At the condition of $n_3 \leqslant n_2$, cladding radius values are 6.0 μm ,4.5 μm and 4.0 μm, respectively. Fig.2 represents the difference between effective refractive index of the fiber and that of the fundamental mode when the cladding radius is infinite. From Fig.2, it is clear that with the decrease of cladding radius b, n is more obviously affected by n_3. Furthermore, from eqs. (1) and (2), the refractive index of external solution can be derived.

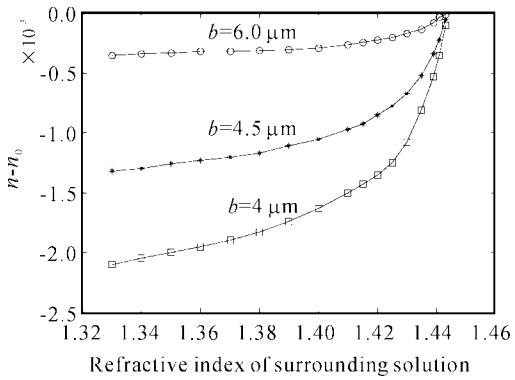

Fig.2 Effective refractive index as a function of outer refractivity for $n_3 \leqslant n_2$

The sensing model used to measure solution refractive index is the F-P cavity as shown in Fig.3, which consists of two FBGs with identical length L and other parameters. On comparison with the ordinary FBG F-P cavity, the fiber cladding between two FBGs is etched to enhance the sensitivity of the model to the external refractive index. When the sensor is placed into solution tested, the refractive index of fiber etched, i.e.n, is not only related to the refractive index of cladding and core, but also affected by the solution refractive index. Furthermore, the change of effective refractive index influences the reflection spectrum of F-P cavity directly. Consequently, the solution refractive index can be measured by analyzing the characteristic of the spectrum.

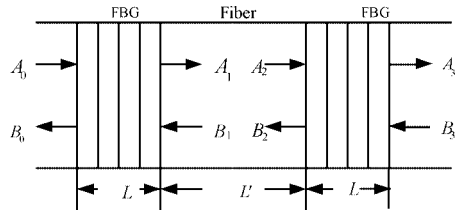

Fig.3 Schematic diagram of refractive index sensing model

The transfer matrix method is used to calculate the output of F-P cavity in the solution. The output can be given by

$$\begin{pmatrix} A_0 \\ B_0 \end{pmatrix} = T \begin{pmatrix} e^{i\varphi} & 0 \\ 0 & e^{-i\varphi} \end{pmatrix} T \begin{pmatrix} A_3 \\ B_3 \end{pmatrix}, \tag{3}$$

where $\varphi=2n\pi L'/\lambda$, L' and n are length and effective refractive index of etched fiber, respectively. And T is the transfer matrix of FBG, which is defined by

$$T=\begin{pmatrix} \cosh(sL)-i\dfrac{\Delta\beta}{s}\sinh(sL) & -i\dfrac{\kappa}{s}\sinh(sL) \\ i\dfrac{\kappa}{s}\sinh(sL) & \cosh(sL)+i\dfrac{\Delta\beta}{s}\sinh(sL) \end{pmatrix},$$

where $\Delta\beta=(2n_{eff}\pi/\lambda)-(2n_{eff}\pi/\lambda_B)$, $s=(\kappa^2-\Delta\beta^2)^{1/2}$, $\lambda_B=2n_{eff}\Lambda$, n_{eff} is the effective refractive index of FBG, κ is coupling coefficient, L is the length of FBG.

Thus, the reflectivity of FBG F-P can be expressed as

$$R_{F-P}=\left|\frac{B_0}{A_0}\right|^2=\left\{\frac{-i\dfrac{\kappa}{s}\sinh(sL)\{e^{i\varphi}[\cosh(sL)-i\dfrac{\Delta\beta}{s}\sinh(sL)]+e^{-i\varphi}[\cosh(sL)+i\dfrac{\Delta\beta}{s}\sinh(sL)]\}}{[\cosh(sL)-i\dfrac{\Delta\beta}{s}\sinh(sL)]^2e^{i\varphi}+\dfrac{\kappa^2}{s^2}\sinh^2(sL)e^{-i\varphi}}\right\}^2. \tag{4}$$

For different values of n, the reflective spectra are shown in Fig.4. The parameters of the simulation are λ_B=1550.5 nm, n_{eff}=1.456, R_{max}=0.9, L=5 mm, L' =10 μm.

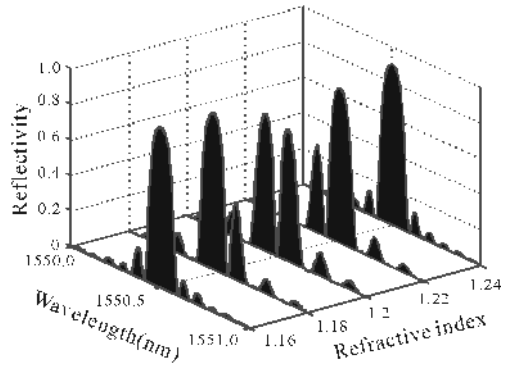

Fig.4 Reflection spectra of Fabry-Perot cavity with different values of *n*.

From the eq.(4), the periodicity of $e^{j\varphi}$ and $e^{-j\varphi}$ can be observed. For a given L', if the spectra keep unchangeable, there is the expression as follows

$$\varphi(n+\Delta n)-\varphi(n)=k\pi(\text{where } k \text{ ia an integer}), \tag{5}$$

i.e. $$\frac{2(n+\Delta n)\pi}{\lambda}L'-\frac{2n\pi}{\lambda}L'=k\pi\cdot \tag{6}$$

When $k=1$, we have

$$\frac{2(n+\Delta n_T)\pi}{\lambda}L'-\frac{2n\pi}{\lambda}L'=\pi\ . \tag{7}$$

Thus, the period can be deduced as

$$\Delta n_T=\frac{\lambda}{2L'}\ , \tag{8}$$

Due to the small range of λ, assuming $\lambda\approx\lambda_B$, hence

$$\Delta n_T=\frac{\lambda_B}{2L'}\ . \tag{9}$$

By substituting parameters of the simulation into Eq. (9), the period $\Delta n_T=0.0775$. Fig.5 shows the reflective spectra corresponding to n=1.2000, 1.2775 (1.2 +Δn_T), 1.3550 (1.2 + 2Δn_T) and 1.4325 (1.2+3Δn_T), respectively. It is readily found that reflective spectrum is periodic, and the period is Δn_T. The simulation results are in good agreement with the theoretical analysis.

In the range of $\Delta\lambda$, $R_{\text{F-P}}=0$ at the position of split point, i. e., Eq.4 can be reduced to

$$e^{i\varphi}[\cosh(\ sL\ )-i(\Delta\beta/s)\sinh(\ sL\ )]+ e^{-i\varphi}[\cosh(\ sL\ )+i(\Delta\beta/s)\sinh(\ sL\ )]=0\ . \tag{10}$$

Therefore, Eq.(10) can be shortened as:

$$\cosh(sL)\cos\varphi+\frac{\Delta\beta}{s}\sinh(sL)\sin\varphi=\cos(\varphi-\varphi_t)=0,$$

where φ_t=arctan[($\Delta\beta$/s)tanh(sL)], φ_t is the transmission phase angle of FBG of a length L[11].

$$\text{Thus},\ \varphi-\varphi_t=m\pi+\frac{\pi}{2}\ , \tag{11}$$

where m is an integer.

Substituting $\varphi=2n\pi L'/\lambda$ into Eq.(11), n is expressed as

$$n=\frac{\lambda}{2\pi L'}\varphi_t+\frac{2m+1}{4L'}\lambda\ . \tag{12}$$

In the range of $\Delta\lambda$, φ_t in Eq.(12) is approximately linear with wavelength as shown in Fig.6.

Consequently, setting

$$\varphi_t=K\lambda+B, \tag{13}$$

where $K=\frac{\varphi_1-\varphi_2}{\Delta\lambda}$, $B=\varphi_1-\frac{\varphi_1-\varphi_2}{\Delta\lambda}\lambda_1$, K and B are constants, and $\varphi_1$and φ_2 are phrases corresponding toλ=λ_1 and λ=λ_2, respectively.

Due to Δn_T=(λ/2L'), substituting (13) into (12), we obtain

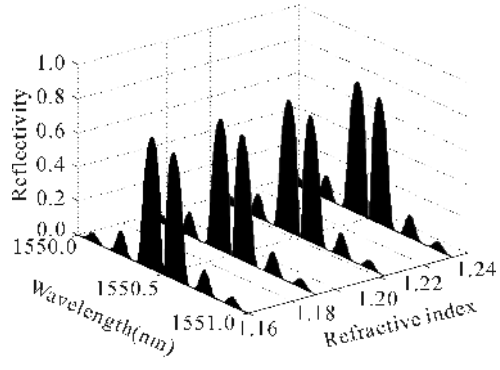

Fig.5 Comparison diagram for the periodicity of spectra

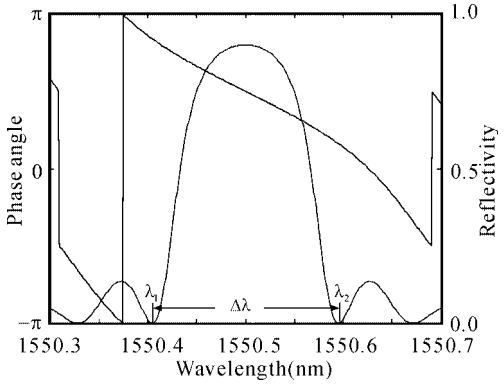

Fig.6 Relationship between φ_t and λ

$$n=\frac{\Delta n_T}{\pi}(K\lambda+B)+\frac{\Delta n_T}{2}+m\cdot\Delta n_T \quad . \tag{14}$$

So the periodicity of n is Δn_T, consistent with analysis as before. Therefore, considering one period, n is approximately linear with λ.Taking m=15, the simulation figure of n and λ is illustrated in Fig.7.

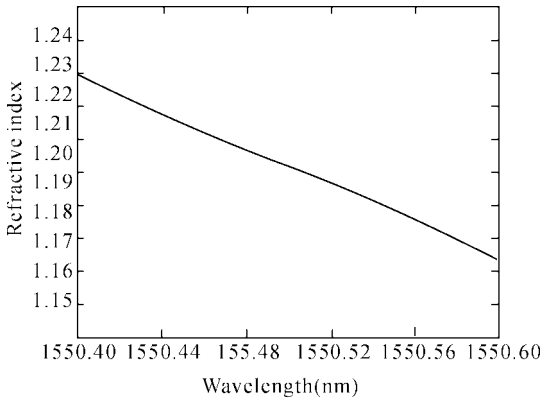

Fig.7 Relationship between *n* and *λ*

From the above analysis, the reflection spectra will be changed with variation of n, and split into two main peaks. The split point shifts periodically. Furthermore, the relationship between split point wavelength and effective refractive index is approximately linear.

In our experiment, the fiber is sealed with paraffin as a protective effect. The fiber is soaked into HF solution with a concentration of 40%. As the time increases, the cladding radius of naked fiber will decrease uniformly. To satisfy sensing requirement, the F-P cavity is taken out after about 35 min. So far, the sensing model of concentration measurement is complete.

The experimental system is shown in Fig.8. The light source is ASE100, output power is 13.5 dBm, the wavelength range is 1528-1610 nm. The reflected light from the FBG F-P cavity is directed into optical spectrum analyzer (EXFO, IQS-5250B, minimum resolution is 0.002 nm).

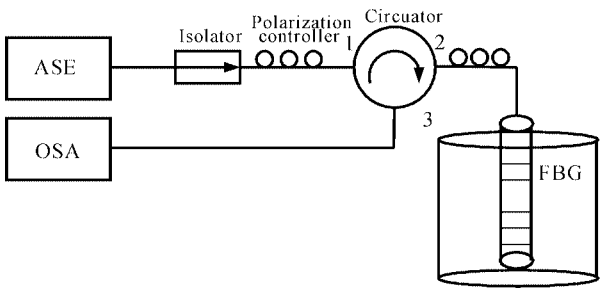

Fig.8 Schematic diagram of experimental system

The central wavelength of FBG in the experimental system is 1549.945 nm at room temperature. The length of F-P cavity composed of two approximately identical FBG with a length of 5 mm, is about 775 μm. When reflective spectrum varies one period, the change of refractive index Δn_T will be 0.001 with the aid of Eq.(9). F-P cavity is put in sucrose solutions with different concentrations from 1% to 59% respectively. The experimental results show that with the variation of concentration, the reflective spectra of FBG F-P cavity will appear a spilt point, and the shift of split point varies periodically.

The original spectra without F-P cavity are shown in Fig. 9. When the concentration of sucrose solution are 5% , 28% and 56% respectively, the experimental results are presented in Fig.10-Fig.12. With the increase of solution concentration , the split point shifts towards short wavelength by comparing Fig.10 and Fig.12. The split point wavelength in Fig.11 and Fig.12 are the same. It suggests that the split point shifts periodically, and the period Δn_T is approximately 0.001, which is basically the same as the theoretical values.

We have recorded 20 experimental data of the split point wavelength, when the concentration of sucrose solution is gradually from 1% to 59% , as shown in Fig.13. It shows that the split point shifts linearly in the bandwidth with the period of Δn_T=0.001.

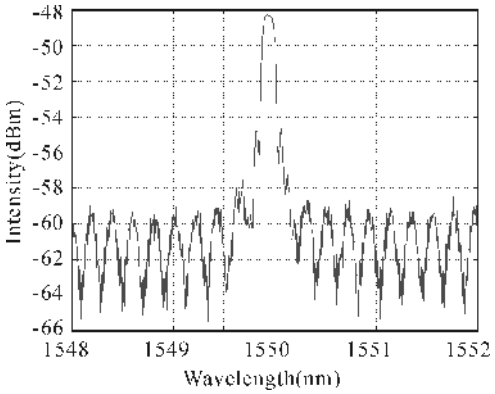

Fig.9 Original spectrum

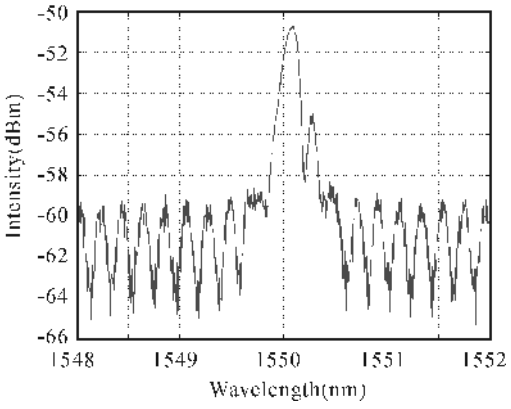

Fig.10 Spectrum when $n_{sucrose}$ =1.3403. n=1.4442

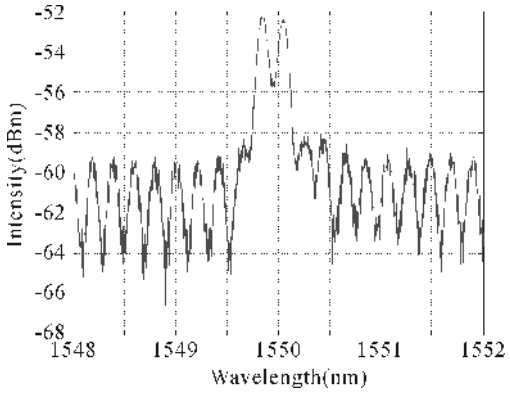

Fig.11 Spectrum when $n_{sucrose}$ =1.3775. n=1.4444

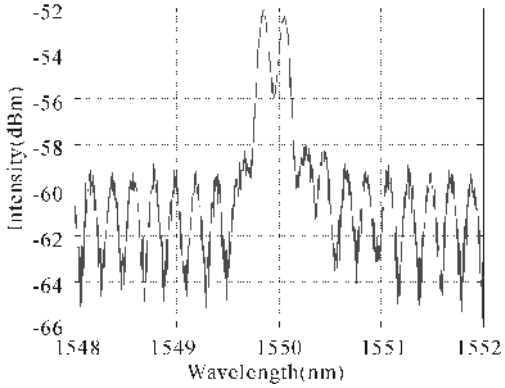

Fig.12 Spectrum when $n_{sucrose}$ =1.4330. n=1.4454

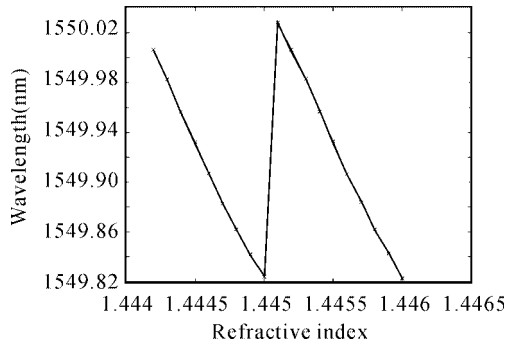

Fig.13 Relationship between effective refractive index and wavelength of split point

This paper studies the characteristics of etched FBG F-P cavity both in theoretical and experiment model. The results show that the etched FBG F-P cavity is sensitive to external refractive index. At constant temperature , when solution concentration varies, the split point wavelength shifts periodically , and it is linear with the refractive index of fiber whose cladding is etched. We use sucrose solution in the experiment, the results show that as the change of fiber effective refractive index is 0.001, the variation of split point wavelength is 0.2 nm, which accords with the theoretical analysis.

References

[1] Guan Shouhua, Yu Qingxu, Song Shide, Chinese Journal of Sensors and Actuators,**18** (2005), 653(in Chinese)

[2] Guo Wengang, Luo Shaojun, Li Yongnan, Tu Chenghou, Lv Fuyun, Acta Photonica Sinica, **36**(2007), 1467(in Chinese)

[3] Wang Yan, Liang Dakai, Ou Qibiao, Zhou Bing, Transducer and Micro system Technologies, **26** (2007), 26(in Chinese)

[4] YU Da-kuan,QLAO Xue-guang, JIA Zhen-an, et al. Journal of Optoelectronics • Laser. **18** (2007),1146(in Chinese)

[5] HUANG Guo-jun, SHAO Jin-yi, WANG Qiu-Lang, et al. Journal of Optoelectronics • Laser, **18** (2007), 0773(in Chinese)

[6] Yun Binfeng, Chen Na, Cui Yiping, Acta Optica Sinica, **26** (2006), 1013(in Chinese)

[7] Xu Junjiao, Li Jie, Rong Huabei, Shi Zhidong, Dong Xiaopeng, Acta Optica Sinica, **28** (2008), 565(in Chinese)

[8] Wei Liang,Yanyi Huang, Yong Xu, Reginald K. Lee, and Amnon Yariv, Applied Physics Letters, **86** (2005), 151122.

[9] David R. Lide. CRC Handbook of Chemistry and Physics (3th Electronic Edition). CRC Press. 2000, E225

[10] Zhang Xia,Xia Yuehui,Huang Yongqing,Ren Xiaomin, Acta Photonica Sinica, **32** (2003), 222(in Chinese)

[11] Liang Meng, Fang Qiang, Wang Yongchang, Journal of Optoelectronics•Laser, **12** (2001), 821.(in Chinese)